

Volatilization of Solid-Phase Polycyclic Aromatic Hydrocarbons from Model Mixtures and Lampblack-Contaminated Soils

Glenn A. Burks and Thomas C. Harmon*

Department of Civil and Environmental Engineering, University of California, Los Angeles 90095-1593

This work summarizes the results from batch experiments investigating the vapor pressure of solid-phase polycyclic aromatic hydrocarbon (PAH) mixtures. Literature regarding the vapor-phase behavior of such systems is sparse because of the relative difficulty in measuring these low volatility compounds. Emerging thermal technologies for remediating soils impacted by such mixtures would greatly benefit from a better understanding of their vapor pressures. An environmentally relevant example of a multicomponent, solid-phase organic contaminant may be associated with lampblack, a sooty byproduct of the oil gasification process employed at former manufactured gas plants (MGPs). PAHs persist at high concentrations in an unspecified state on lampblack and are typically the contaminants of greatest regulatory concern at lampblack-impacted sites. In the first part of this study, three mass ratios for two binary PAH solid combinations were fabricated and studied to determine equilibrium PAH partial pressures. Binary naphthalene–fluorene and naphthalene–anthracene solid samples were fabricated by melt- and solvent-growth crystallization methods to represent dissimilarly and similarly structured pairs, respectively. Results from the model systems demonstrated that the pure-phase vapor pressure was achieved for each component, suggesting that the fabricated multicomponent PAH solids did not behave as a continuous solid solution. Next, partial pressures of several PAHs were measured in the headspace above lampblack-impacted soils from two former MGP sites. Partial pressures ranging from 1% to 60% of the PAH vapor pressures were observed despite the low solid-phase concentrations present in the soils. This result corroborates the results for the fabricated PAH mixtures and implies that continuous solid solutions are unlikely to occur in the field. Thus, vapor pressure–temperature dependency for PAHs in such soils can be estimated using correlations developed for pure PAHs.

Introduction

Polycyclic aromatic hydrocarbons (PAHs) may exist in the environment as multicomponent solid-phase contamination. Relevant examples of nonaqueous-phase solids (NAPS) may be found at former manufactured gas plants (MGPs) in the form of lampblack and solid coal tar.^{1,2} PAHs can comprise a substantial fraction of the NAPS (e.g., as much as 90% of the mass in some coal tars) and are usually the contaminants of greatest regulatory concern owing to their toxicity and/or carcinogenicity.³ Regions of the unsaturated zone impacted by NAPS are typically remediated through excavation followed by relocation, incineration, or treatment by various thermal desorption processes (TDPs).

In TDPs, the addition of heat elevates NAPS vapor pressures. Without this heat, the characteristically low vapor pressures of PAH NAPS would prohibit the use of vapor extraction methods. Examples of *ex situ* TDPs used to clean soils include rotary kilns^{4–7} and batch systems employing microwave heating.⁸ *In situ* TDPs entail extraction and treatment of contaminated vapors. *In situ* methods combine soil-venting and resistive-heating techniques,⁹ thermal blankets that heat the top 0.5 m of soil,^{10,11} or flame-heated pipes buried in the soil.¹² The soil in TDPs may be heated to temperatures where the contaminants are partially or totally liquefied, or above their boiling points, to minimize cleanup times. However, low-temperature TDPs may be employed to reduce energy consumption¹³ or to preserve the natural biota.¹⁴

The behavior of PAH mixtures has recently been studied in the context of understanding mass-transfer phenomena between water and synthetic nonaqueous-phase liquid (NAPL) mixtures^{15,16} and as constituents of coal tar.^{17–22} In most cases, the partitioning of the PAH components into the aqueous-phase conformed to a Raoult's law analogue (i.e., the fugacity coefficients were near unity).^{16,23} Peters et al.²³ studied the phase stability of synthetic multicomponent NAPL–NAPS systems containing PAHs and demonstrated that ideal solubility theory dictates that the NAPL will be a homogeneous liquid if each constituent's mole fraction is less than the solid–liquid reference fugacity ratio at the system temperature. If within the NAPL mixture a constituent's mole fraction exceeds its solid–liquid fugacity ratio, it was implied that the re-solvent precipitated solids comprise separate, pure-phase constituents.

The goal of this work was to elucidate effective sublimation pressures associated with solid PAH mixtures. The literature regarding vapor pressures of individual components over a multicomponent organic solid is currently lacking. The partial pressure at the solid–air interface is an integral part of modeling the mass transfer between the solid and vapor phases, e.g., in low-temperature TDPs, and ultimately influences remediation time requirements and the aqueous-phase concentration in the unsaturated zone. We investigated this issue by measuring the vapor-phase concentration in equilibrium with pure PAHs, fabricated two-component PAH solids, and two lampblack-contaminated soil samples collected at former MGP sites. Esti-

* Corresponding author. Phone: (310) 206-3735. Fax: (310) 206-2222. E-mail: tharmon@ucla.edu.

Table 1. Common Properties and Crystal Dimensions of Selected PAHs

PAH	$T_m/^\circ\text{C}^{24}$	crystal class ^a	a_0/nm	b_0/nm	c_0/nm	α/deg	β/deg	γ/deg	space group
naphthalene	80.6	monoclinic	0.82	0.60	0.87	90°	122°55'	90°	$P2_1/a$
fluorene	113.0	orthorhombic	0.85	1.89	0.57	90°	90°	90°	$Pr2a$
anthracene	217.5	monoclinic	0.86	0.60	1.12	90°	124°43'	90°	$P2_1/a$

^a a_0 , b_0 , and c_0 represent the dimensions of the three independent edges of the unit cell, and α , β , and γ represent the angles between edges b and c, a and c, and a and b, respectively; the space group is the possible groups of symmetry operations for an infinite structure and expresses the totality of the symmetry properties of the crystal structure.³³

mated partial pressures are presented, correlated with temperature, and compared to pure-phase data found in the literature.

Background

Solid–Vapor Equilibria. For multicomponent solids, the partial pressure of the components depends on the state of the solid at a given system temperature and pressure. Two potential states are possible. First, each component may exist as a separate solid phase and impart no thermodynamic effect on the other. This implies that the pure vapor pressure would be attained by each component at equilibrium. Otherwise, the components may form a continuous solid solution, similar to a liquid mixture, in which the thermodynamic properties of the mixture are dependent upon the interactions between components.

For liquid–vapor equilibria, a constituent's partial pressure is proportional to its mole fraction in the liquid times its pure component vapor pressure at a given temperature and is obtained by equating the chemical potential in the liquid phase to that in the gas phase. Real systems necessitate the inclusion of a fugacity coefficient to account for interactions between dissimilar molecules. For ideal systems, the fugacity coefficient is unity, and liquid–vapor equilibria are described by Raoult's law. An analogous relationship may describe a solid–vapor system comprising a multicomponent continuous solid solution in equilibrium with its adjacent vapor.

The experimental protocols discussed below include measuring PAH partial pressures at slightly elevated temperatures. If the system temperature is well below the melting point of a compound, and the heat of sublimation is only a weak function of temperature,²⁴ then the sublimation pressures for the pure PAH samples are expected to correlate with temperature according to the following Antoine-type expression:

$$\log P^s = -\frac{B}{T} + A \quad (1)$$

where $B = \Delta H_{\text{sub}}/(2.3R)$ and $A = \Delta S_{\text{sub}}/(2.3R)$. This expression is commonly used to predict the vapor pressures over solids in environmental applications at or near ambient temperatures. Tabulated values for A and B (experimentally generated) are available for many PAHs.²⁵

Solid PAH Crystal Structure and Growth. The interactions between PAH molecules in the solid phase at the microscopic level ultimately dictate their thermodynamic properties. Solid PAHs are crystalline in structure; that is, their atoms are arranged in a regular three-dimensional array described by three edges and three angles (between the edges). In general, there are seven unique crystal structures.^{26,27} Table 1 lists crystal properties of the PAHs selected for our experiments.

If the components of the solid mixture possess similar enough crystal structures, it is possible to form a continuous solid solution.²⁸ Reisman²⁹ noted that if the lattice constants (axis lengths and angles) of the end members

do not differ by more than 10–15% and the crystal structures are similar, it may be possible to generate a solid solution over the entire range of composition. Because crystal structures vary considerably from one compound to another, solid continuity of a PAH mixture will depend on the compounds involved and their compositions (including impurities) and the conditions of the crystallization process.³⁰

Materials and Methods

Fluorene–naphthalene and anthracene–naphthalene binary mixtures were selected to represent two-component solids comprised of PAHs of dissimilar and similar crystal structure, respectively. Naphthalene and fluorene belong to different crystal classes and space groups (Table 1) and exhibit widely different b_0 and c_0 edge dimensions. Naphthalene and anthracene belong to the same crystal class and space group and exhibit cell dimensions within 10% of one another, with the exception of one cell edge dimension. Another criterion in selecting the PAHs was an observable vapor pressure at ambient conditions.

Vapor pressure data were obtained in batch equilibrium experiments. Certified neat naphthalene, fluorene, and anthracene were used in all experiments (Supelco, Bellefonte, PA). For vapor pressure measurements, pure solid PAH crystals were placed into 40 mL vials sealed with PTFE-lined septa. Certified ACS spectranalyzed hexane (Fisher Scientific, Pittsburgh, PA) was utilized as the solvent for all chemical quantification. Two-component solids were fabricated by melting/cooling (melt-growth) and solvent dissolution/recrystallization (solution-growth) techniques.³¹ Acetone (optima grade, Fisher Scientific) was employed to synthesize the two-component solid samples because of its ability to dissolve large amounts of PAHs and subsequent rapid evaporation. Solid samples were prepared in 1:99, 50:50, and 99:1 mass ratios.

To construct the melted/cooled solid mixtures, 2 mL amber ampules (National Scientific Co., Lawrenceville, GA) were flame-sealed following the insertion and weighing of solid PAH crystals. The solid mixture was immersed in a hot oil bath (Fisher Scientific Isotemp 2013s) at 120 °C for 5 min to melt the crystals. Following the 5 min period, the ampules were removed from the bath and allowed to cool. The solid "mixture" was removed from the 2 mL ampule and placed in a 40 mL vial and allowed to equilibrate in an incubator (± 0.5 °C) at the desired temperature. Naphthalene–fluorene mixtures prepared using the melting protocol were equilibrated at (16, 25 and 33) °C. The same mixtures prepared in the solvent were equilibrated at (16, 25 and 36) °C. All naphthalene–anthracene mixtures were equilibrated at (50, 60 and 70) °C in order to produce measurable anthracene partial pressures. This transfer ensured that pure-phase PAH crystals that had crystallized on the inner walls of the 2 mL ampule did not contribute to partial pressures. A second set of solid mixtures with the same mass ratios was prepared by dissolving the PAHs in acetone and allowing recrystallization to occur while the acetone volatilized.

After a minimum of 24 h of equilibration, 100 μL vapor samples were collected from the 40 mL vials using a gas-tight syringe (Hamilton, Reno, NV) and injected into a gas chromatograph equipped with a flame ionization detector (GC/FID; Hewlett-Packard 5890 II). Separation of PAHs was achieved using a capillary column (J&W Scientific, DB-17, 0.5 μm film thickness, 30 m \times 0.53 mm i.d.). Helium and nitrogen served as the carrier and makeup gases, respectively. Residual PAH adsorbed on the inside of the syringe was collected in a 1–2 μL hexane rinse and analyzed on the GC. This residual mass accounted for less than 10% of the total observed mass.

Samples of representative two-component PAH solids fabricated by the melting/cooling method were diluted in hexane and analyzed using a gas chromatograph/mass spectrometer (GC/MS; Finnigan, Sunnyvale, CA) system to identify potential thermal decomposition products. A 30 m DB-5, 0.25 mm i.d. column (J&W Scientific, Folsom, CA) was used to separate the compounds with helium as the carrier gas.

Density-induced composition variations are a potential artifact of the melt-growth protocol. To measure the homogeneity of the 99:1 fluorene–naphthalene solid samples generated by the melting/cooling method, each sample was carefully sliced horizontally into three disklike shapes and diluted in hexane. Diluted samples were injected (1 μL) into the GC/FID, and the resultant concentrations were used to estimate local solid mixture compositions.

Soil samples were collected from soil borings taken from lampblack-impacted zones at two different former MGP sites in the Los Angeles area. The samples, Aliso soil (a moist, fine to medium grain sand) and the El Centro soil (a wet, silty clay), were delivered to a certified laboratory (AETL, Burbank, CA). There a portion of each sample was subjected to Soxhlet extraction and a battery of standard analyses [EPA 8310 for PAHs, 8260B for volatile organics, M8015G for total petroleum hydrocarbons (gasoline), M8015D for TPH as diesel/heavy hydrocarbons] to estimate the soil concentrations for an array of organic contaminants, including PAHs. A second portion of the soil was then analyzed at UCLA for PAH vapor concentrations. Prior to analysis, both soil samples were air-dried in a fume hood (1 day), then transferred to a desiccator, and stored for about 1 week to reduce the moisture content. The Aliso soil was relatively dry following desiccation, while the more claylike El Centro soil retained a significant amount of water. Each soil sample was split into six vials and sealed using mininert valves (Supelco). Roughly, 150 g of Aliso soil was placed into a 120 mL vial and 20 g of El Centro soil was placed into a 25 mL vial (differences due to soil mass availability), and each was equilibrated in an oven maintained at 70 $^{\circ}\text{C}$ (± 0.5 $^{\circ}\text{C}$).

PAHs partial pressures were identified and quantified by injecting 100 μL of the sample headspace into the GC/MS with an extended temperature ramp (35–275 $^{\circ}\text{C}$ over 50 min). Differences in headspace concentrations were observed as a function of equilibration time in several preliminary samples, suggesting a rate-limited approach to the vapor–soil equilibrium. Results reported here are for 1 month. While this time appeared to be sufficient for achieving equilibrium in the drier, granular Aliso soil, equilibrium was difficult to conclusively quantify for the wetter El Centro clay. Thus, the headspace measurements reported here may not be representative of the true equilibrium vapor concentration in these real soils, but they are expected to be well within an order of magnitude of the true concentration.

Table 2. Methods and Measured Vapor Pressures at 20 $^{\circ}\text{C}$ for Naphthalene and Fluorene from the Literature and for This Work

	P°/Pa	ref
Naphthalene		
manometry	14.26	36
effusion	10.8	37
effusion	12.26	38
effusion	10.42	39
gas saturation	10.9	40
gas saturation	10.64	41
gas saturation	11.33	42
gas saturation (HPLC/UV)	10.4	32
generator column (HPLC)	10.4	43
GC–RT	7.91	36
batch headspace/GC-FID	10.39 (± 0.31)	this work ^a
Fluorene		
manometry	0.127	44
effusion	0.087	37
gas saturation (HPLC/UV)	0.079	32
generator column (HPLC)	0.08	43
batch headspace/GC-FID	0.083 (± 0.002)	this work ^a

^a Average of five samples (\pm standard deviation).

Table 3. Final Compositions of 99:1 Fluorene–Naphthalene (F–N) Melted Solid Samples^a

sample	original F–N ratio	average final ratio	% average deviation
vial 1, slice 1	0.0104	0.000 51	15.11
vial 2, slice 1	0.0102	0.000 62	5.88
vial 3, slice 1	0.0113	0.000 62	10.43
vial 1, slice 2	0.0104	0.000 56	4.60
vial 2, slice 2	0.0102	0.001 10	10.29
vial 3, slice 2	0.0113	0.000 94	3.17
vial 1, slice 3	0.0104	0.000 67	7.99
vial 2, slice 3	0.0102	0.000 77	5.80
vial 3, slice 3	0.0113	0.001 18	4.42

^a Slice 1 represents the top portion of the cylindrical solid sample, slice 2 the middle portion, and slice 3 the bottommost portion.

Results and Discussion

Pure-component vapor pressures were measured to verify method accuracy and reproducibility. The measured pure-component vapor pressures for naphthalene and fluorene at 20 $^{\circ}\text{C}$ were found to be in reasonable agreement with literature values (Table 2) with good precision (standard deviation of about 3%). The wide range of reported values in the literature (nearly a factor of 2) underscores the difficulty in measuring vapor pressures of relatively low volatility compounds.

Each 99:1 fluorene–naphthalene solid sample formed by the melting/cooling exhibited a relatively homogeneous composition (Table 3). However, the original (targeted) N/F ratio was roughly 20 times greater than the ratio actually achieved. The tendency of the more volatile compound (naphthalene) to volatilize at a faster rate during the melting process is the most likely cause of this result. Thus, the mass ratios for the purported 99:1 fluorene–naphthalene and anthracene–naphthalene samples prepared by the melting/cooling process were substantially higher with respect to fluorene and anthracene.

Constituent vapor pressures over fluorene–naphthalene and anthracene–naphthalene solid mixtures prepared using both fabrication methods were measured at the equilibration temperatures noted previously. In all cases, measured partial pressures agreed with pure constituent vapor pressures. Experimental data for each compound are summarized in the form of eq 1 and shown in Figures 1–3.

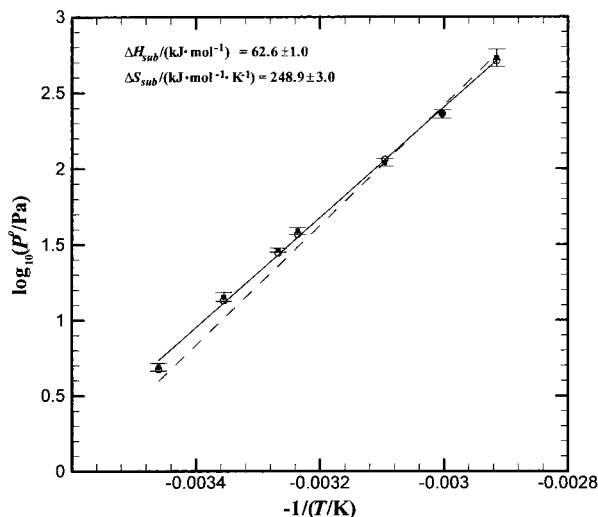


Figure 1. Naphthalene sublimation pressure $\log(P^\circ/\text{Pa})$ correlation for temperatures 15–70 °C: squares, binary samples from this work (error bars represent experimental standard deviation); circles, pure naphthalene samples from this work (error bars encompassed by symbols); dashed line, pure naphthalene; solid line, linear regression for binary samples. Thermodynamic properties shown ($\pm 95\%$ CI) are based on the regression constants (eq 1) for the binary data.

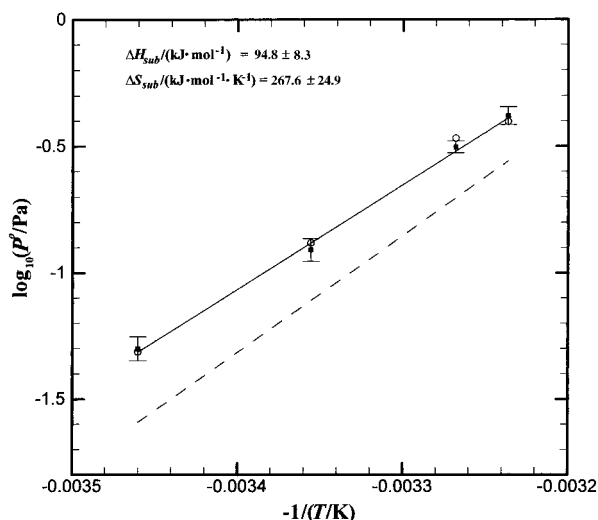


Figure 2. Fluorene sublimation pressure $\log(P^\circ/\text{Pa})$ correlation for temperatures 15–35 °C: squares, binary samples from this work (error bars represent experimental standard deviation); circles, pure naphthalene samples from this work (error bars encompassed by symbols); dashed line, pure naphthalene; solid line, linear regression for binary samples. Thermodynamic properties shown ($\pm 95\%$ CI) are based on the regression constants (eq 1) for the binary data.

For comparison, pure-phase experimental data collected in this investigation and in the study conducted by Sonnefeld et al.³² are also shown. The fact that this observation was true even for the dilute components (e.g., naphthalene as <1% by mass) provides strong evidence of a failure to achieve continuous solid mixtures by either fabrication method.

When the solid mixtures were synthesized utilizing the melting/cooling method, byproducts were formed as a result of molecular decomposition. 1-Ethyl-2,3-dimethylbenzene and 1,2,3,4-tetramethylbenzene were identified as the predominant byproducts. Additional byproducts were observed on the chromatogram but not identified. Because

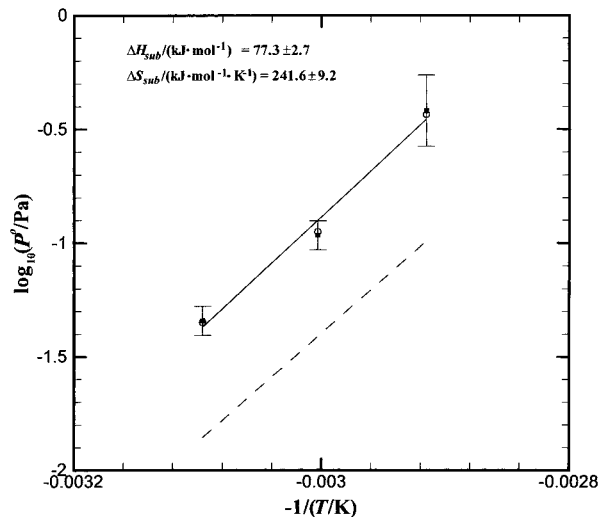


Figure 3. Anthracene sublimation pressure $\log(P^\circ/\text{Pa})$ correlation for temperatures 15–35 °C: squares, binary samples from this work (error bars represent experimental standard deviation); circles, pure naphthalene samples from this work (error bars encompassed by symbols); dashed line, pure naphthalene; solid line, linear regression for binary samples. Thermodynamic properties shown ($\pm 95\%$ CI) are based on the regression constants (eq 1) for the binary data.

the formation of a continuous solid solution requires components with nearly identical crystal structure, these byproducts may have precluded the formation of an ideal solid mixture.

PAH solid mixture synthesis using the solvent-growth crystallization method presumably avoids complications associated with byproduct formulation. To entirely dissolve the anthracene in the 99:1 anthracene–naphthalene solid samples, more than double the amount of solvent necessary for the fluorene–naphthalene samples was required, which greatly increased the time required to completely evaporate the solvent. Because of its very small fraction, nearly all of the naphthalene also volatilized during the evaporation process. Consequently, naphthalene was not detected in the vapor samples taken from the 99:1 anthracene–naphthalene solid samples. Analysis of the 99:1 anthracene–naphthalene solid-phase sample confirmed the absence of detectable naphthalene.

Crystal defects caused by trapped solvent molecules, twinning, and straining are also possible explanations for the failure to grow a continuous solid solution. The number of solvent or other foreign molecules required to disrupt continuous solid solution formation is dependent upon the system, is very difficult to determine, and was beyond the scope of this study. Twinning is described by the formation of zones with similar structure but different orientation and is caused when the individual molecules improperly stack within the crystal lattice.³³ A crystal may experience physical straining when subjected to outside forces. Advanced electron microscopic techniques are required to investigate these issues.³³

Thermodynamic ramifications of crystal defects caused by impurities and varying surface-to-bulk-phase properties have been discussed.³⁰ One potentially significant consequence is the dissimilarity of the enthalpy of fusion at the crystal surface to that in the bulk phase. In this case, because the partial pressure adjacent to the surface of the crystal is dependent upon the surface properties, the observed partial pressure would be different from that observed adjacent to the bulk-phase crystal. This consequence may be reflected in the mass-transfer coefficient

Table 4. Partial Pressures of Several PAHs Measured Using GC/MS Headspace Analysis for Two Lampblack-Contaminated Soils at 70 °C

soil and PAH component	soil concd ^a /mg·kg ⁻¹	average observed partial pressure/Pa	average % of measured pure PAH std ^b	average % of reported vapor pressure ^c
Aliso (<i>n</i> = 10) ^d				
naphthalene	1850	ADL	> 10	> 10
fluorene	37	0.53 (0.11) ^e	15 (3)	6 (1)
phenanthrene	172	0.46 (0.08)	16 (3)	19 (3)
anthracene	32	0.057 (0.016)	42 (12)	56 (16)
fluoranthene	84	0.010 (0.005)	9 (4)	9 (4)
pyrene	100	0.011 (0.004)	42 (15)	15 (5)
El Centro				
naphthalene (<i>n</i> = 12)	134000	ADL	> 10	> 10
fluorene (<i>n</i> = 12)	566	0.12 (0.03)	3 (0.8)	1.4 (0.4)
phenanthrene (<i>n</i> = 12)	11000	0.65 (0.38)	18 (11)	27 (16)
anthracene (<i>n</i> = 2)	714	0.064 (0.016)	36 (9)	63 (15)
fluoranthene (<i>n</i> = 9)	8060	0.034 (0.022)	18 (12)	32 (21)
pyrene (<i>n</i> = 9)	9350	0.043 (0.032)	45 (34)	58 (44)

^a American Environmental Testing Laboratory (AETL) EPA Method 8310. ^b Measured using the same method with pure PAH standards. ^c Calculated from $P^{\circ}-T$ correlations.³² ^d Ten samples for Aliso soil and varied with PAH for El Centro soil; see the explanation in the text. ^e Parentheses denote standard deviation values.

observed in a dynamic system (e.g., TDP). However, in batch equilibrium experiments this affect is likely imperceptible because sufficient time is allowed to overcome this resistance.

Pure-phase crystals formed on the inner walls of several of the sampling vials through condensation followed by crystallization directly from the vapor phase and may have contributed to observed PAH partial pressures. Crystals were observed on the inner walls of the 1:99 and 50:50 anthracene–naphthalene sample vials at temperatures of (60 and 70) °C. However, evidence of crystal formation was not detected at any temperature for the 99:1 anthracene–naphthalene samples nor for any of the fluorene–naphthalene samples. It is postulated that, for the cases where crystal formation was observed, a sufficient concentration of naphthalene and/or anthracene was present in the air phase to facilitate crystal growth on the vial walls. Given the linearity of the data in Figure 1, it is presumed that this potential artifact did not affect the results.

Figure 1 illustrates the close agreement between the naphthalene sublimation pressure correlation developed in this investigation to that of Sonnefeld et al.³² However, the previous results consistently predict fluorene and anthracene vapor pressures less than those measured in this work. Given that good agreement exists between experimental pure-phase and multicomponent data collected in this study, this discrepancy is most likely due to differences in experimental procedure. During the sampling process, the more strongly adsorbing fluorene and anthracene may have left an overrepresented mass on the inside walls of the gas-sampling syringe. Sonnefeld et al. utilized a gas saturation method that eliminates contributions by adsorption. The gas saturation method is generally regarded as the most accurate method for determining the vapor pressures for low volatility compounds.³² However, this method cannot be applied in a system consisting of binary solid mixtures because of loss of mass and consequential variation in mass ratios between individual components in the solid mixture. Greater experimental error is also expected for the less volatile compounds in which the detection limit on the GC (0.05 ng) was closely approached. Regardless of these explanations, the parallel pure-phase standards provided the necessary check to show that the pure-phase vapor pressure was achieved above the binary mixtures.

PAH vapor-phase concentrations for the soil samples were quantified for five PAHs and are reported as partial

pressures in Table 4. Also reported are the solid-phase PAH concentrations as well as the estimated fraction of the pure PAH vapor pressure that was achieved. It is important to note that the most volatile of the PAHs (naphthalene) is reported in terms of its lowest possible concentrations, because vapor-phase concentrations of this compound were well above the method detection limit and would require a substantial amount of dilution to be more accurately quantified. Thus, it appeared that naphthalene was actually present in amounts several times greater than the lower bounds shown in Table 4.

Overall, the results for the contaminated soils corroborated those from the model PAH mixtures in that the PAHs achieved high partial pressures relative to their measured solid-phase concentrations. This result is in spite of unanswered questions regarding the adequacy of the equilibration period and uncontrolled losses to the bottle/valve apparatus, which would tend to lower the observed vapor-phase concentrations. This result takes on still more weight when one notes that numerous other organic compounds were found in substantial quantities in the soil samples (e.g., TPH-diesel 1700 mg/kg and TPH-gasoline 2000 mg/kg for the Aliso sample and many others). The presence of these compounds would tend to depress the PAH vapor-phase concentrations still more if mixtures were present in the soils. Thus, one can conclude that independent PAH behavior occurs in some contaminated soils.

With respect to the solid-phase concentrations, the El Centro soil was found to contain substantially greater concentrations of PAHs than the Aliso soil. Nevertheless, the Aliso soil exhibited partial pressures comparable to those observed for the more contaminated soil. For example, roughly 50% of anthracene's vapor pressure was observed in both soils despite the fact that the Aliso and El Centro solid-phase anthracene concentrations were roughly 30 and 700 mg/kg, respectively. Roughly 20% of phenanthrene's vapor pressure was achieved in both soils despite the fact that their respective solid-phase concentrations were roughly 200 and 11 000 mg/kg. These results provide further support of the notion of independent solid-phase PAH behavior in contaminated soils.

Environmental Implications

At some distance away from the heat source in a TDP, or in a low-temperature TDP, a solid organic mixture (or

aggregated pure phases) will remain solid as dictated by the compounds' melting points. Hence, the sublimation pressure of each component in such a process must be determined to estimate removal times. Environmentally relevant solid-phase examples containing PAHs (e.g., lamp-black) involve complex mixtures of both similar and dissimilar compounds. While this work does not eliminate the possibility of the existence of continuous PAH solid solutions in the environment, it suggests that the likelihood of such an occurrence is small. Therefore, the temperature dependency of such contaminants can be estimated using P - T relationships developed for pure compounds. At near-ambient temperatures, sublimation pressure-temperature correlations for the most common PAHs have been assembled from experimentally generated data.²⁵ Also, a general correlation developed by Mackay et al.³⁴ requires only the melting and boiling points of a compound to estimate its vapor pressure at a given temperature and may be applied at any temperature.

Acknowledgment

The authors gratefully acknowledge UCLA undergraduate Carina Chen for assistance in collecting batch vapor pressure data, Ed Ruth for overseeing the GC/MS work, and Masood Hosseini (Sempra Energy) for locating the former MGP facility soils.

Literature Cited

- Remediation Technologies Inc. *Management of Manufactured Gas Plant Sites*; Gas Research Institute: GRI-87/0260.1, Chicago, IL, 1987.
- Electric Power Research Institute. *Chemical and Physical Characteristics of Tar Samples from Selected Manufactured Gas Plant (MGP) Sites*, Final Report for Research Project 2879-12; EPRI TR-102184; Palo Alto, CA, 1993.
- Swartz, R. W.; Schults, D. W.; Ozretich, R. J.; Lamberson, J. O.; Cole, F. A.; Dewitt, T. H.; Redmond, M. S.; Ferraro, S. P. Sigma-PAH—A Model to Predict the Toxicity of Polynuclear Aromatic Hydrocarbon Mixtures in Field-Collected Sediments. *Environ. Toxicol. Chem.* **1995**, *14*, 1977–1987.
- Thurnau, R. C. Low-Temperature Desorption Treatment of Co-Contaminated Soils—TCLP As an Evaluation Technique. *J. Hazard. Mater.* **1996**, *48*, 149–169.
- Thurnau, R. C.; Manning, J. A. Low-Temperature Desorption Applications of a Direct-Fired Rotary Kiln Incinerator. *J. Air Waste Manage. Assoc.* **1996**, *46*, 12–19.
- Fox, R. D.; Alperin, E. S.; Huls, H. H. Thermal Treatment for the Removal of Pcb's and Other Organics from Soil. *Environ. Prog.* **1991**, *10*, 40–44.
- Lighty, J. S.; Eddings, E. G.; Lingren, E. R.; Deng, X. X.; Pershing, D. W.; Winter, R. M.; McClennen, W. H. Rate-Limiting Processes in the Rotary-Kiln Incineration of Contaminated Solids. *Combust. Sci. Technol.* **1990**, *74*, 31–49.
- Kawala, Z.; Atamanczuk, T. Microwave Enhanced Thermal Decontamination of Soil. *Environ. Sci. Technol.* **1998**, *32*, 2602–2607.
- Webb, S. W.; Phelan, J. M. Effect of Soil Layering on NAPL Removal Behavior in Soil-Heated Vapor Extraction. *J. Contam. Hydrol.* **1997**, *27*, 285–308.
- Vinegar, H. J. Thermal Desorption Cleans Up PCB Sites. *Power Eng.* **1998**, *102*, 43–45.
- Iben, I. E. T.; Edelstein, W. A.; Sheldon, R. B.; Shapiro, A. P.; Uzgirir, E. E.; Scatena, C. R.; Blaha, S. R.; Silverstein, W. B.; Brown, G. R.; Stegemeier, G. L.; Vinegar, H. J. Thermal Blanket For in-Situ Remediation of Surficial Contamination—a Pilot Test. *Environ. Sci. Technol.* **1996**, *30*, 3144–3154.
- Harmon, T. C. (ENV America Inc.). *Pilot Test Report: Soil Venting Thermal Desorption Pilot (SVTD) Test*, ENV America Project Number SCG-01-T038; Southern California Gas Co.: Los Angeles, 1999.
- Sullivan, T. P. Thermal Desorption: the Basics. *Chem. Eng. Prog.* **1999**, *95*, 49–56.
- Bonten, L. T. C.; Grotenjuis, T. C.; Rulkens, W. H. Enhancement of PAH Biodegradation in Soil by Physicochemical Pretreatment. *Chemosphere* **1999**, *38*, 3627–3636.
- Ortiz, E.; Kraatz, M.; Luthy, R. G. Organic Phase Resistance to Dissolution of Polycyclic Aromatic Hydrocarbon Compounds. *Environ. Sci. Technol.* **1999**, *33*, 235–242.
- Mukherji, S.; Peters, C. A.; Weber, W. J. Mass Transfer of Polynuclear Aromatic Hydrocarbons from Complex DNAPL Mixtures. *Environ. Sci. Technol.* **1997**, *31*, 416–423.
- Ramaswami, A.; Luthy, R. G. Mass Transfer and Bioavailability of PAH Compounds in Coal Tar NAPL—Slurry systems. 1. Model Development. *Environ. Sci. Technol.* **1997**, *31*, 2260–2267.
- Ramaswami, A.; Ghoshal, S.; Luthy, R. G. Mass Transfer and Bioavailability of PAH Compounds in Coal Tar NAPL—Slurry Systems. 2. Experimental Evaluations. *Environ. Sci. Technol.* **1997**, *31*, 2268–2276.
- Luthy, R. G.; Ramaswami, A.; Ghoshal, S.; Merkel, W. Interfacial Films in Coal Tar non-Aqueous Phase Liquid–Water System. *Environ. Sci. Technol.* **1993**, *27*, 2914–2918.
- Peters, C. A.; Luthy, R. G. Coal Tar Dissolution in Water-Miscible Solvents—Experimental Evaluation. *Environ. Sci. Technol.* **1993**, *27*, 2831–2843.
- Lee, L. S.; Rao, P. S. C.; Okuda, I. Equilibrium Partitioning of Polycyclic Aromatic Hydrocarbons from Coal Tar into Water. *Environ. Sci. Technol.* **1992**, *26*, 2110–2115.
- Lane, W. L.; Loehr, R. C. Estimating the Equilibrium Aqueous Concentrations of Polynuclear Aromatic Hydrocarbons in Complex Mixtures. *Environ. Sci. Technol.* **1992**, *26*, 983–990.
- Peters, C. A.; Mukherji, S.; Knightes, C. D.; Weber, W. J. Phase stability of multicomponent NAPLs containing PAHs. *Environ. Sci. Technol.* **1997**, *31*, 2540–2546.
- Schwarzenbach, R. P.; Gschwend, P. M.; Imboden, D. M. *Environmental Organic Chemistry*; Wiley: New York, 1993.
- Allen, J. O.; Sarofin, A. F.; Smith, K. A. Thermodynamic Properties of Polycyclic Aromatic Hydrocarbons in the Subcooled Liquid State. *Polycycl. Aromat. Compd.* **1999**, *13*, 261–283.
- McKie, D.; McKie, C. *Crystalline Solids*; Nelson: London, 1974.
- Moore, W. J. *Basic Physical Chemistry*; Prentice-Hall: Englewood Cliffs, NJ, 1983.
- Swalin, R. A. *Thermodynamics of Solids*; Wiley: New York, 1962.
- Reisman, A. *Phase Equilibria: Basic Principles, Applications, Experimental Techniques*; Academic Press: New York, 1970.
- Ubbelohde, A. R. *Melting and Crystal Structures*; Clarendon Press: Oxford, 1965.
- Strickland, R. F. *Kinetics and Mechanism of Crystallization*; Academic Press: New York, 1968.
- Sonnefeld, W. J.; Zoller, W. H.; May, W. E. Dynamic Coupled-Column Liquid Chromatographic Determination of Ambient Temperature Vapor Pressures of Polynuclear Aromatic Hydrocarbons. *Anal. Chem.* **1983**, *55*, 275–280.
- Wright, J. D. *Molecular Crystals*; Cambridge University Press: Cambridge, 1995.
- Mackay, D.; Bobra, A.; Chan, D. W.; Shiu, W. Y. Vapor Pressure Correlations for Low Volatility Environmental Chemicals. *Environ. Sci. Technol.* **1982**, *16*, 645–649.
- Wyckoff, R. W. G. *Crystal Structures*; Krieger: Huntington, NY, 1981.
- Bidleman, T. F. Estimation of Vapor Pressures for Nonpolar Organic Compounds by Capillary Gas Chromatography. *Anal. Chem.* **1984**, *56*, 2490–2496.
- Bradley, R. S.; Cleasby, T. G. The vapour pressure and lattice energy of some aromatic ring compounds. *J. Chem. Soc.* **1953**, 1690–1692.
- Radchenko, L. G.; Kitaigorodskii, A. I. Vapor pressure and heat of sublimation of naphthalene, biphenyl, octafluoronaphthalene, decafluorobiphenyl, acenaphthene and α -nitronaphthalene. *Russ. J. Phys. Chem.* **1974**, *48*, 2702–2704.
- De Kruij, C. G.; Kuipers, T.; Van Miltenburg, J. C.; Schaake, R. C. F.; Stevens, G. The vapour pressure of solid and liquid naphthalene. *J. Chem. Thermodyn.* **1981**, *13*, 1081–1086.
- Sinke, G. C. A method for measurement of vapor pressures of organic compounds below 0.1 Torr. Naphthalene as reference substance. *J. Chem. Thermodyn.* **1974**, *6*, 311–316.
- Macknick, A. B.; Prausnitz, J. M. Vapor pressure of high-molecular weight hydrocarbons. *J. Chem. Eng. Data* **1979**, *24*, 175–178.
- Grayson, B. T.; Fosbraey, L. A. Determination of the Vapor Pressure of Pesticides. *Pest. Sci.* **1982**, *13*, 269–278.
- Wasik, S. P.; Miller, M. M.; Tewari, Y. B.; May, W. E.; Sonnefeld, W. J.; DeVoe, H.; Zoller, W. H. Determination of the vapor pressure, aqueous solubility, and octanol/water partition coefficient of hydrophobic substances by coupled generator column/liquid chromatographic methods. *Res. Rev.* **1983**, *85*, 29–42.
- Osborn, A. G.; Douslin, D. R. Vapor pressures and derived enthalpies of vaporization of some condensed-ring hydrocarbons. *J. Chem. Eng. Data* **1975**, *20*, 229–231.

Received for review February 19, 2001. Accepted April 23, 2001. This work was sponsored by the National Science Foundation (BES-9502170). Supplemental funding was provided by the UCLA Center for Environmental Risk Reduction (CERR). The results have not been subjected to agency review and an official endorsement should not be inferred.

JE0100544